Functional characterization and FTIR-based 3D modeling of full length and truncated forms of Scorpio maurus venom phospholipase A 2

Najeh Krayem, Goetz Parsiegla, Hélène Gaussier, Hanen Louati, Raida Jallouli, Pascal Mansuelle, Frédéric Carrière, Youssef Gargouri

Functional characterization and FTIR-based 3D modeling of full length and truncated forms of *Scorpio maurus* venom phospholipase A₂

Najeh Krayem[1], Goetz Parsiegla[2], Hélène Gaussier[2], Hanen Louati[1], Raida Jallouli [1],

Pascal Mansuelle[3], Frédéric Carrière[2], Youssef Gargouri[1*]

[1] : Laboratoire de Biochimie et de Génie Enzymatique des Lipases, ENIS, Université de Sfax, route de Soukra 3038, BP 1173 Sfax-Tunisia.

[2] : Aix Marseille Université, CNRS, UMR7282 Enzymologie Interfaciale et Physiologie de la Lipolyse, 31 Chemin Joseph Aiguier, 13402 Marseille Cedex 20, France.

[3] : Institut de Microbiologie de la Méditerranée, CNRS FR3479, 31 Chemin Joseph Aiguier, 13402 Marseille Cedex 20, Aix Marseille Université, France.

[*]Correspondence address : Pr. Youssef Gargouri, Laboratoire de Biochimie et de Génie Enzymatique des Lipases, ENIS, Université de Sfax, route de Soukra 3038, BP 1173 Sfax-Tunisia. Tel /Fax : + 216 74 67 50 55

E-mail: ytgargouri@yahoo.fr

Keywords :

Abbreviations

Sm-PLGV : Phospholipase A_2 purified from *Scorpio maurus* venom glands.

rPLA$_2$(+5) : recombinant phospholipase A_2 containing the whole gene transcript either Long and short chains linked by the penta-peptide.

rPLA$_2$(-5) : recombinant phospholipase A_2 in which the penta-peptide insert is deleted.

Long chain : recombinant phospholipase A_2 constructed only by one chain, truncated at the beginning of the penta-peptide insert.

hbPLA$_2$: honey bee phospholipase A_2

sPLA$_2$: secreted phospholipase A_2

p-BPB : p-bromophenacyl bromide

FTIR : Fourier Transform Infrared Spectroscopy

Egg-PC : Egg Phosphatidyl-choline

diC$_{12}$-PC : 1,2-dilauroyl-sn-Glycero-3-phosphocholine

diC$_{12}$-PE : 1,2-dilauroyl-sn-Glycero-3-phosphoethanolamine

PS : diacyl-L-α-phosphatidyl-L-serine

PG : diacyl-L-α-phosphatidyl-DL-glycerol

Abstract

Background: Heterodimeric phospholipase A_2 from venom glands of Tunisian scorpion *Scorpio maurus* (Sm-PLGV) had been purified. It contains long and short chains linked by a disulfide bridge. Sm-PLGV exhibits hemolytic activity towards human erythrocytes and interacts with phospholipid monolayers at high surface pressure. The investigation of structure-function relationships should provide new clues to understand its activity.

Methods: Molecular cloning of Sm-PLGV and heterologous expression in *Escherichia coli* of three recombinant forms was used to determine the role of the short chain on enzymatic activity. Infrared spectroscopy assisted 3D model building of the three recombinant constructs (phospholipases with and without the penta-peptide and Long chain only) allowed us to propose an explanation of the differences in specific activities and their interaction with various phospholipids.

Results: Nucleotide sequence of Sm-PLGV encodes 129 residues corresponding to the Long chain, the penta-peptide and the short chain. Although recombinant phospholipases without and with the penta-peptide have different specific activities, they display a similar substrate specificity on various phospholipid monolayers and similar bell-shaped activity profiles with maxima at high surface pressure. The absence of the short chain reduces significantly enzymatic and hemolytic activities. The 3D models pointed to an interaction of the short chain with the catalytic residues, what might explain the difference in activities of our constructs.

Conclusion: Infrared spectroscopy data and 3D modeling confirm the experimental findings that highlight the importance of the short chain for the Sm-PLGV activity.

General significance: New informations are given to further establish the structure-function relationships of the Sm-PLGV.

1. Introduction

Phospholipases A_2 (PLA_2) catalyze the hydrolysis of the ester function at the *sn*-2 position of glycerophospholipids, to produce free fatty acids and lysophospholipids [1]. They are widely distributed in pancreatic juices and many tissues [2, 3] as well as in the venom produced by many animals[4].

The PLA_2 superfamily comprises four main types of enzymes: secreted ($sPLA_2$), cytosolic ($cPLA_2$), calcium independent ($iPLA_2$), and platelet activating factor acetyl hydrolase (PAF-AH). $sPLA_2$ are the most common type found in both vertebrates and invertebrates and are subdivided into twelve groups based on primary sequences alignments, disulfide bond pattern and their biochemical properties [5, 6]. $sPLA_2$ have a low molecular weight (13–15 kDa), usually contain 6–8 disulfide bonds [7], share a His/Asp dyad with a conserved histidine and require the presence of calcium for their catalytic activity.

Snake venoms contain high amounts of $sPLA_2$ that belong either to group I (Elapidae and Hydrophidae snakes) or to group II (Crotalidae and Viperidae snakes). They are among the best characterized components of these venoms in terms of structure and function. $sPLA_2$ play an important role in the digestion of prey and exhibit a wide spectrum of pharmacological activities like myotoxicity, neurotoxicity, inflammatory, hemolytic, and anticoagulant effects [8], anti-bactericidal properties [9, 10] as well as anti-tumoral activity [11, 12].

Group III PLA_2 have been identified in many other species [13-15] like scorpion [16-19], gila monster [20], lizards [21] and human [22]. They are involved in inflammation [23, 24], apoptosis [25] and cancer [26, 27]. Group III $sPLA_2$ contain ten cysteines and are composed of one or two chains. They are only distantly related to group I and II, but have a highly similar Ca^{2+} binding loop and active site region [22].

Scorpion venom $sPLA_2$ belongs to group III and is composed of a long enzymatic chain and a short covalently fixed C-terminal chain generated after the release of five residues (penta-peptide) during the maturation processes [28]. Different members of group III $sPLA_2$ from scorpion venoms have been purified such as $HfPLA_2$ from *Heterometrus fulvipes* [29], $MtPLA_2$ from *Mesobuthus tumulus* [19] Imperatoxin (IpTxi) [16] and Phospholipin from *Pandinus imperator* [30], Phaiodactylipin from *Anuroctonus phaiodactylus* [17], Heteromtoxin (HmTx) from *Heterometrus laoticus* [18], Hemilipin from *Hemiscorpius lepturus* [27] and Sm-PLVG from *Scorpio maurus* [31].

Structural models of the long chain of group III sPLA$_2$ have been built based on the available crystal structure of bee venom sPLA$_2$ which has a high sequence identity in this major part of the fold but not in the smaller C-terminal extension. In all models, the overall fold comprises three α-helices, an antiparallel β-sheet of two strands and a calcium binding loop. Even if biochemical characteristics of scorpion sPLA$_2$ have been studied intensively, few modeled structures have been published. Like in other sPLA$_2$, the scorpion transcript codes for a long enzymatic N-terminal chain, a connecting penta-peptide followed by a short C-terminal extension. The long chain is stabilized by four disulfide bonds and is responsible for the enzyme activity. The short one contains a free cysteine after the scissile penta-peptide which is suggested to form a disulfide bond with a cysteine at the end of the long chain to covalently connect both parts even after excision of the connecting penta-peptide. The function of this small chain is less clear and its sequence may vary in composition and in length between different species. In some cases, it has a high content in hydrophobic residues and may fold into an anti-parallel β-sheet, making it ideal for specific tissue targeting [32].

Scorpio maurus belongs to the Scorpionidae family found in the Mediterranean, Middle East, Saudi Arabia and Jordan regions [31]. Reports on pharmacological properties of the venom of this scorpion identified various toxins [33, 34]. Recently, a phospholipase A$_2$ named Sm-PLGV has been purified from its venom glands. It has a specific activity of 5500 U/mg on phosphatidylcholine substrate at 47°C and pH 8.5, in the presence of 8 mM NaTDC and 12 mM CaCl$_2$. Moreover, Sm-PLVG exhibits an hemolytic activity towards human, rabbit and rat erythrocytes. This hemolytic activity is related to its ability to interact with phospholipid monolayers at high surface pressure [31].

In this study, we report the molecular cloning of Sm-PLGV and its sequence comparison with other known group III sPLA$_2$. To determine the impact of the penta-peptide insert and the importance of the short chain on enzymatic activity, we produced in *Escherichia coli* three recombinant forms: rPLA$_2$(+5) containing the whole gene transcript with long and short chains linked by the penta-peptide, rPLA$_2$(-5) in which the penta-peptide insert is deleted but long and short chains have been fused to a single covalent chain, and Long chain which is composed only by the long N-terminal chain, truncated at the beginning of the penta-peptide insert. We compared the biochemical and interfacial properties of these recombinant forms with those of native Sm-PLGV phospholipase purified from *Scorpio maurus* venom. Structural models of these three variants were built based on the X-ray

structure of bee venom PLA$_2$ and their individual FTIR spectra to find structural explanations for the observed enzyme properties.

2. Material and methods

2.1   Reagents

All restriction endonucleases and DNA modifying enzymes were from Promega (France) and were used according to the manufactures' protocols. Chemicals were obtained from commercial sources. Guanidine hydrochloride (Amresco, catalogue E424); l-cysteine (ACROS organics), chromatography materials (Q-sepharose), Sodium dodecyl sulfate (SDS), acrylamide, ammonium persulfate, N,N,N',N'-tetramethyl ethylenediamine (TEMED), β-mercaptoethanol and Coomassie brilliant blue R-250 were obtained from Bio-Rad. NaCl, CaCl$_2$, Tris–HCl, Bovine serum albumin (BSA), sodium taurodeoxycholate (NaTDC), ethylenediaminetetraacetic acid (EDTA), Triton X100, egg phosphatidylcholine (egg-PC), 1,2-dilauroyl-sn-glycero-3-phosphocholine   (diC$_{12}$-PC),   1,2-dilauroyl-sn-glycero-3-phosphoethanolamine (diC$_{12}$-PE), diacyl-L-α-phosphatidyl-L-serine (PS), diacyl-L-α-phosphatidyl-D,L-glycerol (PG), proteins markers for molecular masses, isopropyl-thio-β-D-galactopyranoside (IPTG), β-cyclodextrin, p-bromophenacyl bromide (p-BPB), 5,5′-Dithiobis 2-nitrobenzoic acid and ampicillin were purchased from Sigma Aldrich (St. Quentin-Fallavier, France).

2.2   Animals

Scorpions (*Scorpio maurus*) were collected alive from the area of Agareb (Sfax, Tunisia). Only the last segments of metasoma (telsons) were used as starting material.

2.3   Bacterial strains, plasmids and media

E. coli strain XL1Blue was used for cloning the gene encoding Sm-PLGV phospholipase. *E. coli* strain BL21(DE3) served as the expression host for the rPLA$_2$(+5), rPLA$_2$(-5) and Long chain gene constructs. *E. coli* strains were grown in LB medium, supplemented with 100 μg.mL^{-1} ampicillin whenever a plasmid was present. The PGEM-T Easy and pET21a(+) plasmids were used as cloning and expression vectors, respectively. PCR products were purified using Wizard PCR Preps DNA purification System (Promega).

2.4 cDNA synthesis

Total RNA was extracted from 10 telsons of *Scorpio maurus* using the Total RNA isolation system KIT (Promega). For reverse transcription (RT), total RNA (5 µg) was converted to cDNA by M-MuLV Reverse Transcriptase using polydT as primer. RT-PCR conditions were 25°C for 10 min, 37°C for 60 min and 70°C for 10 min.

2.5 Cloning of Sm-PLGV cDNA

Polymerase chain reaction (PCR) of 35 cDNA ends was performed on the obtained *S. maurus* cDNA using the specific primers PSPLGV: 5'ATGGTAGATTTGGCAAGAAGATG3' and CtPLGV: 5'CTAGTCTTTGTAGCTCTTTTCC3'. These primers were designed according to the nucleotide sequence of phospholipin from *Pandinus imperator* venom [30] and phaiodactylipin from *Anuroctonus phaiodactylus* [17]. The PCR protocol consisted of 35 cycles at 94°C (60 s), 52°C (60 s), 72°C (60 s) respectively and a final extension at 72°C for 10 min. PCR products were analyzed on agarose gels 1%. The appropriate DNA band was purified using the gel extraction kit and cloned into EcoRI-cut and dephosphorylated PGEM-T Easy vector, using the PGEM-T Easy Vector system, according to the manufacturer's protocol (Promega). *E. coli* strain XL1 Blue cells were then transformed with the ligated vectors. Recombinant colonies were selected on LB-ampicillin (100 µg.mL^{-1}) plates supplemented with IPTG and X-Gal. The presence of the appropriate insert was monitored by restriction analysis. DNA products were analyzed on a standard 1% agarose gel and their sequences determined with the dideoxynucleotide chain termination method according to a cycle sequencing protocol using thermosequenase (Amersham Pharmacia Biotech).

2.6 Construction of expression plasmids

The DNA sequence of the complete *S. maurus* PLA$_2$ gene allowed the design of new forward primer 5'GGAATTCCATATGTTTCTTATATGGGGAGGGACC3'corresponding to the N-terminus of the mature protein and reverse primer 5'CCGCTCGAGCTAGTCTTTGTAGCTCTTTTCC3' corresponding to the C-terminus of the protein. They were synthesized to amplify the gene construct rPLA$_2$(+5) coding for whole unprocessed peptide chain of the Sm-PLGV phospholipase. The primer 5'GGAATTCCAT ATGTTTCTTATATGGGGAGGGACC3' and a reverse primer 5'CCGCTCGAGCTAACTGTTACATGTCACAACATAGC3' were used to obtain the Long chain construct. An overlap PCR was used to obtain the gene construct rPLA$_2$(-5) in which the

7

connecting penta-peptide is deleted. Four primers were synthesized: 5'GGAATTCCATATGTTTCTTATATGGGGAGGGACC3' and

5'CCATTTTCACATCCTGCATCACTGTTACATGTCACAAC3' to amplify the sequence coding for the long chain up to the location of the penta-peptide and 5'GTTGTGACATGTAACAGTGATGCAGGATGTGAAAATG3' and

5'CCGCTCGAGCTAGTCTTTGTAGCTCTTTTTCC3' to amplify the sequence coding for the short chain after the penta-peptide. The PCR products obtained with each pair of primers were purified and used as matrices to amplify the rPLA$_2$(-5) construct with the primers corresponding to the 5' and 3' ends of the entire Sm-PLGV cDNA. The purified constructs and the expression vector pET21(a)+ were digested with NdeI and XhoI restriction enzymes. After dephosphorylating the expression vector with calf intestinal alkaline phosphatase for 30 min at 37°C and 20 min at 60ºC, each insert was ligated into pET21a(+) to obtain the expression vectors pET21a-rPLA$_2$(+5), pET21a-rPLA$_2$(-5) and pET21a-Long chain which were used in the transformation of *E. coli* BL21(DE3) cells and protein expression. The presence of the appropriate inserts was verified by restriction analysis and their DNA sequences determined as mentioned above.

2.7 Expression and purification of rPLA$_2$(+5), rPLA$_2$(-5) and Long chain

Transformed cells were grown in LB medium containing 100 µg.mL^{-1} ampicillin at 37ºC to an absorbance at 600 nm of about 0.6 to 0.8 and then protein expression was induced with IPTG which was added to a final concentration of 1 mM. After induction, cells were incubated for an additional 5 h at 37ºC and harvested by centrifugation for 15 min at 12000 rpm. Recombinant proteins were obtained as inclusion bodies and were renaturated and purified following a protocol adapted from Bhat and al., 1991[35] and Karray and al, 2014 [36].

Harvested cells were resuspended in 50 mL of resuspension buffer R (50 mM Tris–HCl pH 8.0, 50 mM NaCl, 1 mM EDTA, 0.5 mM PMSF) to obtain a final cell suspension of 20% (w/v). Triton X-100 and sodium deoxycholate were added to 0.4% (w/v) final concentration and the mixture was stirred for 20 min at 4°C. Cell disruption was performed by sonication using an MSE Sonyprep 150 at full power; 15 seconds on and 15 seconds off for 15 cycles. After centrifugation at 10000 rpm for 10 min at 4°C, the sonication process was repeated with increased concentrations of both Triton X-100 and sodium deoxycholate at 0.8% (w/v). The solid pellet obtained after centrifugation (10000 rpm for 10 min) was first washed with the buffer R containing 1% Triton X-100, then subsequently rinsed with buffer without Triton X-

100. Finally, the pellet was solubilized in buffer R containing 6 M guanidine hydrochloride and 5% β-mercaptoethanol (25 mL) and stirred overnight at 4°C. The solubilized proteins (~0.8 mg/mL) were obtained by centrifugation at 10000 rpm for 10 min at 4°C.

Protein refolding was performed following the procedure previously described by Karray and al., [36]. Denatured recombinant phospholipases were refolded by dialyzing 4-times 25 mL of the protein solution (~0.8 mg/mL) against 2 L of buffer A (20 mM Tris–HCl pH 8.0, 5 mM $CaCl_2$, 5 mM L-cysteine, 0.6 M guanidine hydrochloride) at 4°C for 48 h. Then precipitate was removed by centrifugation at 10000 rpm for 10 min and guanidine hydrochloride was removed from the protein solution by dialysis against 2 L of buffer B (20 mM Tris–HCl pH 8.0, 20 mM NaCl, 5 mM $CaCl_2$) at 4°C overnight. The solution was filtered (0.45 µm) and loaded on a Q-Sepharose anion exchange column equipped with an absorbance monitoring at 280 nm and previously equilibrated with buffer B. The column was washed using the same buffer until the absorbance dropped to zero. Then, proteins were eluted with a linear gradient of 20 mM to 400 mM NaCl in buffer B. All three recombinant proteins were eluted between 200 mM and 300 mM NaCl. The fractions (1.5 ml) were collected and analyzed for the presence of phospholipase activity. The fractions with phospholipase activity showing a single band in SDS-PAGE analysis were pooled and concentrated to about 1 mL using an Amicon concentrator (YM 5 membrane).

2.8 MALDI-TOF mass spectrometry analysis

Global molecular mass of *Sm*-PLVG, $rPLA_2$(-5), $rPLA_2$(+5) and Long chain was determined by by matrix-assisted laser desorption ionization time-of-flight (MALDI ToF) mass spectrometry using a Microflex II instrument (Bruker Daltonics,Bremen, Germany) in a positive linear mode. Range was set from 3600 to 40,000 Da and pulse ion extraction was set to 160 ns. External mass calibration was done just before the acquisition of samples using protein calibration standard I (Bruker Daltonics, Germany). A saturated solution of α-Cyano-4-hydroxycinnamic acid (HCCA) in 70% acetonitrile/30% water 0.1% TFA was used as matrix. Deposits were made onto a MALDI Target plate according to a dried droplet method and each dried spot was then desalted three times by adding, and removing immediately after, 1.5 µl of 0.1% TFA/water followed by a supplementary addition of matrix.

2.9 Sm-PLGV deglycosylation

Enzymatic deglycosylation of Sm-PLGV was performed at 37 °C for 3 h using 20 µg of purified Sm-PLGV and 1000 units of PNGase F (from Promega). After the reaction, the molecular mass of the treated enzyme was analyzed by MALDI-ToF.

2.10 Hydrolysis of phospholipid monolayers

The monolayer study was performed as described previously by Pattus et al., [37]. Prior to each experiment the Teflon trough used to form the phospholipid monomolecular films was cleaned with water before being gently brushed with distilled ethanol and washed again with tap water. The aqueous subphase contained 10 mM Tris–HCl pH 8.0, 150 mM NaCl, 20 mM CaCl$_2$, 1 mM EDTA and 0.5 mM β-cyclodextrin. The buffer was prepared with double distilled water and filtered through a 0.22 µm Millipore filter. Any residual surface-active impurities were removed before each assay by sweeping and suction of the surface. Experiments were performed at room temperature with a KSV-2200 barostat (KSV Helsinki) using a ''zero order'' Teflon trough equipped with a mobile Teflon barrier, which was used to compensate for the substrate molecules removed from the film by enzyme hydrolysis, thus maintaining the surface pressure constant. The latter was measured using a Wilhelmy plate (perimeter 3.94cm) attached to an electro-balance, which was connected in turn to a microprocessor controlling the movements of the mobile barrier. The subphase of the reaction compartment was continuously agitated with a 2-cm magnetic stirrer moving at 250 rpm. The enzyme solution was injected through the film over the stirrer with a Hamilton syringe. The surface area of the reaction compartment was 120 cm^2 and its volume was 120 ml. The reservoir compartment was 148 mm wide and 249 mm long. Hydrolysis of phospholipid monolayers by phospholipases results in the formation of lysophospholipid and free fatty acid. With medium (C12) chain phospholipid substrates, these products are water-soluble and desorb rapidly from the monolayer, which results in a surface pressure decrease. With lon chain substrates, the presence of β-cyclodextrin in the bulk phase allows the solubilization of lipolysis products. In both cases, phospholipase activity was deduced from the mobile barrier displacement to keep the surface pressure constant. The surface covered by the barrier was converted into substrate molecules based on compression isotherms of phospholipid monolayers at the air-water interface. Activities were expressed as the number of moles of substrate hydrolyzed by unit time and unit surface of the reaction compartment of the ''zero-order'' trough for appropriate sPLA$_2$ concentration.

10

2.11 Covalent inactivation of phospholipases

Chemical modification of Sm-PLGV, rPLA$_2$(+5) and rPLA$_2$(-5) enzymes was performed by incubating each protein with 1 mM p-bromophenacyl bromide (p-BPB) dissolved in 0.5% dimethylsulfoxide. Incubation was carried out at 4°C for 1 h and then the excess of the reagent was removed by dialysis against Tris-buffer pH 8. The absence of enzyme activity was checked by pH-stat method and modified enzymes were used in hemolysis test. In parallel, controls were run without inhibitor under the same conditions.

2.12 Reaction of DTNB (5,5′-Dithiobis(2-nitrobenzoic acid) with native and recombinant phospholipases

We check disulfude bond formation in the native and the three recombinant phospholipases by probing free thiols using 5,5-dithio-bis-(2-nitrobenzoic acid) (DTNB), as described previously by Gargouri et al., 1988 [38]. 20 mM of DTNB was useful for spectrophotometric determination of sulfhydryl groups in different phospholipases. A 1 mL cuvette was filled with 600 µL of 0,1M Tris-HCl buffer pH 8.0 containing 0.1 mg/mL of Sm-PLGV, rPLA$_2$(-5), rPLA$_2$(+5) or Long chain and a 40-60 molar excess of DTNB. The value of the absorbance of the mixtures as compared with a blank containing no enzymes was recorded versus time. The number of sulfhydryl groups was calculated from the maximal absorbance, using molar extinction coefficient value of 13600 at 412 nm for thiopyridone. At the same time, residual phospholipase activity was measured on samples.

2.13 Hemolysis assay

Hemolytic activity of the pure recombinant proteins was tested using human erythrocytes [31]. Freshly collected blood samples were immediately mixed with anticoagulant, to prevent blood coagulation. To obtain a pure suspension of erythrocytes, 1 mL of whole blood was made up to 20 mL in phosphate buffered saline (PBS pH 7.4) and centrifuged at 1500 rpm for 5 min at 4°C. The supernatant and buffy coats were removed by gentle aspiration, and the above process was repeated two more times. Erythrocytes were finally suspended in PBS to make 1% solution for the hemolytic assay. Various amounts of pure rPLA$_2$(+5), rPLA$_2$(-5) and Long chain were added to red blood cells suspension which were gently mixed, incubated at 37°C for 30 min, and then centrifuged at 1500 rpm for 5 min at 4°C. The absorbance of the supernatants was determined at 545 nm to measure the extent of red blood cell lysis and hemoglobin release. Positive control (100% hemolysis) and

negative control (0% hemolysis) were also run by incubating erythrocytes in PBS containing 1% Triton X-100 and PBS alone, respectively.

2.14 Phospholipase A$_2$ assay

Phospholipase activity was measured titrimetrically with a pH-stat under the standard conditions: at pH 8.5 and 50°C, in the presence of 8 mM NaTDC and 12 mM CaCl$_2$ using 1% w/v egg phosphatidylcholine (egg-PC) as substrate. One PLA$_2$ unit corresponds to the liberation of one µmole of fatty acids (FFA) per minute.

2.15 Determination of protein concentration

Protein concentration was determined according to the Bradford method [39] using BSA as a reference.

2.16 FTIR spectroscopy

The FTIR absorption spectra of the purified phospholipases (50 µg) were recorded between 400 and 4000 cm^{-1} using an Analect Instruments fx-6 160 spectrometer. Spectral analysis of the amide I band was performed with Spectra manager (Jasco) after a baseline correction from 1500 to 1800 cm^{-1}. A Fourier self-deconvolution considering a FWHM initial estimation of 18 cm^{-1} was applied.

2.17 Molecular modeling

Construction of 3D-models of the phospholipase variants was performed using the Swissmodel web server for the N-terminal catalytic domain (Long chain up) to its last disulfide bond (Cys100) [40] and manually, using the WinCoot (v. 7.2.1) protein model building and verification program for the C-terminal extensions [41]. N- and C-terminal parts were fused and additionally refined by several rounds of a combination of i) simple energy minimization (3 to 5 cycles) under default parameters and predefined disulfide bridges added as constrains using the Refmac program (v. 5.8.0151) from the CCP4 program package [42, 43], ii) the ModRefiner program from the I-Tasser server which allowed to obtain more native fold characteristics [44, 45] and iii) manual correction of the Ramachandran plot using the structure regularization functions of Wincoot with Ramachandran constraints turned on. The quality of the models was assessed with the Wincoot program, which checked for Ramachandran plot and geometry outliers. Illustrations of the structures were produced using

the PyMol program [46]. The electrostatic surface was generated using the APBS program [47]. Dipole moments and vectors were calculated using the dipole.py script of the Chimera molecular modeling system[48].

3. Results

3.1 Sequencing of *Scorpio maurus* PLA$_2$ gene and recombinant proteins purification

The *Scorpio maurus* PLA$_2$ gene presentend in Fig.1, that encodes both chains, the long and the short chain separated by a penta-peptide Lys-Arg-Ser-Ser-Arg, is transcribed into a single mRNA, which is processed during maturation, in quite the same way as initially demonstrated for the case of IpTxi [16], phospholipin from *Pandinus imperator* [30] and MtPLA$_2$ from *Mesobuthus tumulus* [28]. The sequence is composed of 387 nucleotides, starting at residue Phe 1 and ending at residue Asp 129, just before the stop codon.

The nucleotide sequence coding the rPLA$_2$(+5) is formed by the whole sequence starting at nucleotide 1 to the nucleotide 387. The Long chain sequence starts at nucleotide 1 to nucleotide 321. The rPLA$_2$(-5) sequence is formed by the Long chain (nucleotide 1 to 321) and the short one (337 to 387) without the penta-peptide sequence (figure 1). Open reading frames of 387 bp, 372 bp and 321 bp encoding proteins of 129, 124 and 107 amino acids and theoretical molecular masses of 14637 Da,14022 Da and 12168 Da were obtained for rPLA2(+5), rPLA2(-5) and Long chain, respectively. The expressed proteins in *E. coli* BL21DE3, which were present in inclusion bodies, were purified after protein refolding using anion exchange chromatography on Q-Sepharose (data not shown).
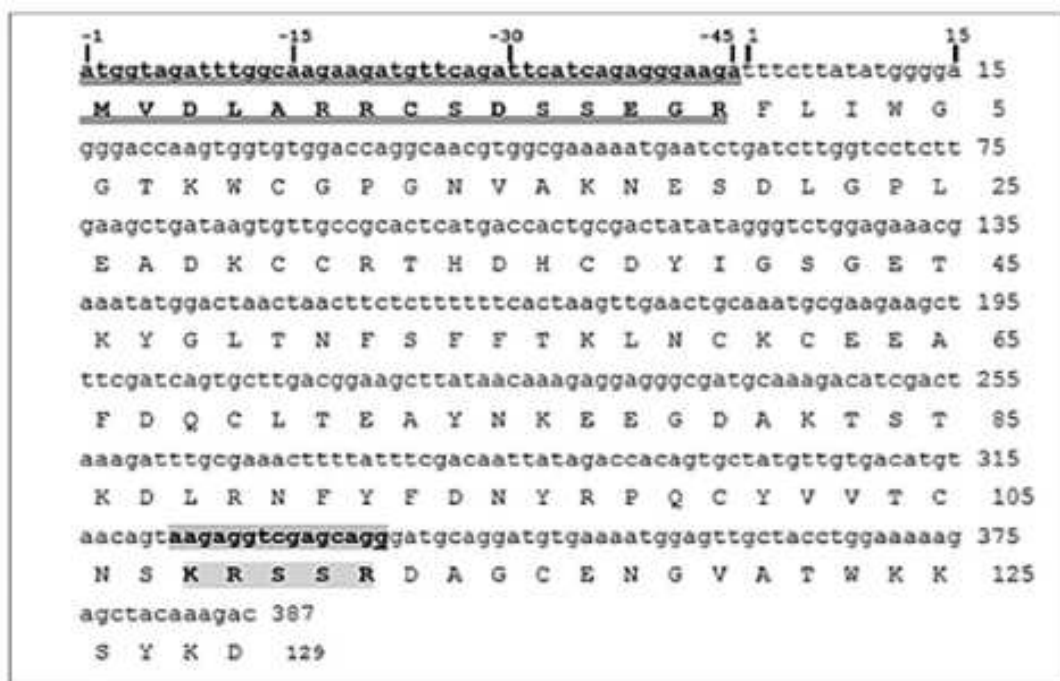
Figure 1: Nucleotide sequence of Sm-PLGV gene encoding the mature phospholipase and the deduced amino acid sequence (Long chain: F1 to S107; short chain: D113 to D129). The signal peptide is double underlined). The cleavable penta-peptide is shown as a grey box.

We determined the molecular masses of native Sm-PLGV and the different recombinant constructs using MALDI-TOF mass spectrometry (Figure 2 and Table 1).

Table 1: Theoretical and experimental masses and specific activities of native and recombinant phospholipases. Phospholipase activity was measured using egg-PC 1% as substrate under standard conditions.

Construct	Sm-PLGV	rPLA$_2$(-5)	rPLA$_2$(+5)	Long chain
Theoretical molecular mass (Da)	14637	14144.63	14759.33	12168
MALDI-ToF data (Da)	15155	14144	14776	Not determined
AS (U/mg)	5500	1500	450	50

Figure 2: The MALDI-TOF mass spectrometry of **(A)** Sm-PLGV, **(B)** rPLA$_2$(-5),**(C)** rPLA$_2$(+5) and **(D)** Long chain

Enzymatic deglycosylation of Sm-PLGV was performed and its molecular mass was analyzed by MALDI-ToF. The treated Sm-PLGV have the same molecular mass as the untreated enzyme. This observation can be explained by the small size of the carbohydrate group or by its inaccessibility to PNGase F (data not shown).

3.2 Effect of temperature on phospholipase activity and stability of rPLA$_2$(-5), rPLA$_2$(+5) and Long chain

Phospholipase activity was tested under standard conditions at temperatures ranging from 25 to 60°C with the pH stat technique (Fig. A.3). The highest activity was observed at 50°C for all constructs. Specific activity of the full lenght rPLA$_2$(+5) was reduced to 450 U/mg which was lower than native Sm-PLGV and rPLA$_2$(-5), both without penta-peptide 'KRSSR' (specific activities 5500 U/mg and 1500 U/mg respectively). Even though the Long chain variant contains the catalytic site, its activity was only 50 U/mg, which suggests that the short chain plays a role in catalytic efficiency.

Thermostability of rPLA$_2$(+5), rPLA$_2$(-5) and Long chain was investigated by measuring the residual activity after 30 min of incubation at various temperatures ranging

15

from 25 to 65°C (Fig. B.3). Native Sm-PLGV and the variants presented a similar behavior towards the temperature. Phospholipase activity decreased with increasing temperature and was lost at 65°C. We could notice that Long chain alone is less stable than the other constructs towards temperature.
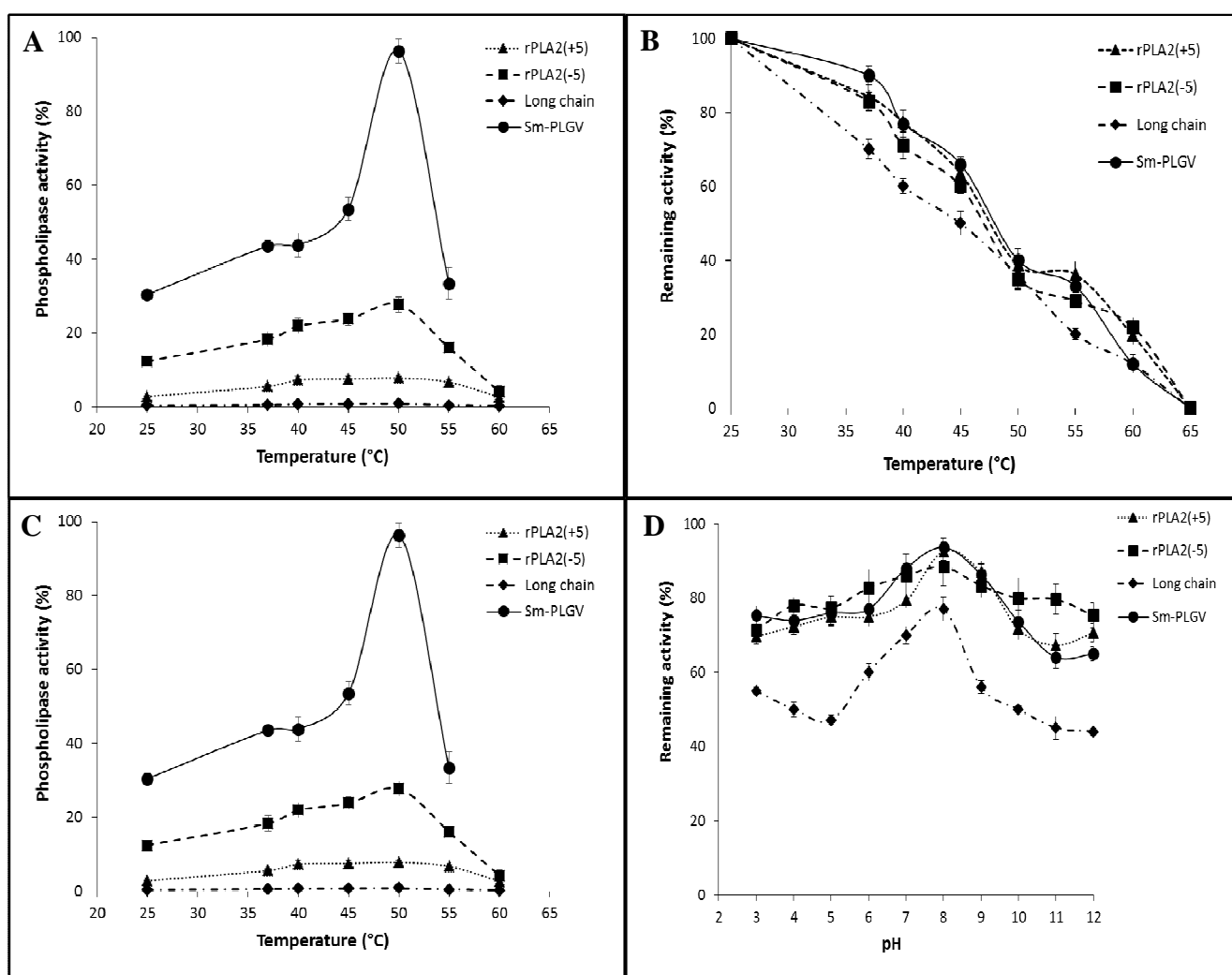

Figure 3: Effect of pH and temperature on rPLA$_2$(-5), rPLA$_2$(+5) and Long chain activity and stability. Sm-PLGV was taken as a control for a comparative study. The enzymatic activity was measured at various temperatures at pH 8.5 **(A)** and various pH **(C)** in the presence of 12 mM CaCl$_2$ and 8 mM NaTDC. **(B)** The enzyme stability towards the temperature was estimated from residual activity measurements performed after 30 min

incubation of 0.1 µM of each enzyme at different temperatures at pH 8.5. **(D)** The pH stability of phospholipases was checked after incubation of each enzyme at various pH for 30 min. Residual phospholipase activity was measured under standard conditions using egg-PC 1% as substrate corresponding approximately to 13 mM.

3.3 Effect of pH on phospholipase activity and stability of the purified rPLA$_2$(-5), rPLA$_2$(+5) and Long chain

Phospholipase activity was measured at 50°C at different pH values using egg-PC dispersion as substrate. The pH vs activity profile of purified phospholipases is shown in Fig. C.3. Like native Sm-PLGV, all variants are active in a pH range from 7.0 to 9.0 with an optimum at pH 8.5. This optimum pH of activity is also similar to that of *M. tamulus* venom phospholipase MtPLA$_2$ [49].

Stability at different pH was studied by incubating the enzymes with different buffers at pH values ranging from 3.0 to 12.0 and at 4°C before assessing their activity under standard conditions. Like Sm-PLGV, all variants were found to be stable between pH 3.0 and 12.0, with their maximum activity between pH 8.0 and 9.0 (Fig. D.3). rPLA$_2$(+5) and rPLA$_2$(-5) kept more than 70% and 60% of their activity after incubation at basic and acid pH respectively. Long chain was generally less stable over this pH range, but shared the same pH profile.

3.4 Ca^{2+} and bile salts dependence of the purified rPLA$_2$(-5), rPLA$_2$(+5) and Long chain

It is well established that Ca^{2+} is essential in secreted phospholipases for both, activity and binding to their substrates [50]. We measured rPLA$_2$(-5) , rPLA$_2$(+5) and Long chain activities under standard conditions in the presence of increasing Ca^{2+} concentrations (data not shown). As expected, all variants were inactive in the presence of a Ca^{2+}-chelator like EDTA and their catalytic activity increased with Ca^{2+} concentrations. But while activity of rPLA$_2$(-5) rose linearly with [Ca^{2+}] increase right from the start, with rPLA$_2$(+5) a threshold concentration of 8 mM had to be exceeded first. In all cases the highest specific activity was observed with the highest tested concentration of Ca^{2+} at 12 mM. Similar results were obtained with sPLA$_2$ purified from *Anuroctonus phaiodactylus* and *M. tamulus* venoms [17-19] and two snake venom PLA$_2$: CC-PLA$_2$ from *Cerastes cerastes* and MVL-PLA$_2$ from *Macrovipera lebetina* wich stain active up to 10 mM Ca^{2+} [51]. Moreover, we measured rPLA$_2$(-5), rPLA$_2$(+5) and Long chain phospholipase activities under standard conditions with

increasing concentrations of NaTDC (data not shown). Bile salts were required for rPLA$_2$(-5), rPLA$_2$(+5) and Long chain activities and their highest activity was observed at 8 mM NaTDC. Similar to their thermal activity, rPLA$_2$(-5) exhibited the highest activity in the presence of bile salts, while Long chain was lowest.

3.5   Kinetic parameters of native and recombinant phospholipases

The kinetic parameters (apparent Km, kcat and the catalytic efficiency kcat/Km) of each enzyme were determined. We measured the specific activities as a function of PC concentration for the different enzymes under standard conditions. Then, apparent Km, turnover kcat and catalytic efficiency (kcat/Km) were estimated from Lineweaver–Burk plots (data not shown) for each enzyme (Table 2).

Sm-PLGV presents the highest kcat/Km value. In contrast, the presence or the absence of the penta-peptide decreases significantly the catalytic efficiency. The lowest kcat/Km was obtained when the short chain was removed from the native structure (Long chain). This result undergoes the importance of the short chain in the enzyme expression.

Table 2: Apparent kinetic parameters of Sm-PLGV and its recombinant forms

	V$_{max}$ (µmol/min/mg)	Km (mM)	kcat (s^{-1})	kcat/Km (s^{-1}.mM^{-1})
Sm-PLGV	5500	2,3	1410	613
rPLA$_2$(-5)	1500	4	352	88
rPLA$_2$(+5)	450	5,5	110	20
Long chain	50	2,5	10	4

3.6   Reaction of DTNB (5,5′-Dithiobis(2-nitrobenzoic acid) with native and recombinant phospholipases

To check disulfude bond formation in the native and three recombinant enzymes, we measured free thiols using DTNB. We showed that Sm-PLGV, rPLA$_2$(-5) and rPLA$_2$(+5) have no free SH. In contrast with Long chain, one free SH was modified without loss of its activity (data not shown).

3.7   Hemolytic activity of the purified rPLA$_2$(-5), rPLA$_2$(+5) and Long chain

As native Sm-PLGV showed direct hemolytic activity, we tested if its recombinant variants have this property despite their difference in specific activity. Hemolytic activity was tested with human erythrocytes suspension. Fig. A.4 shows that 100 % of hemolysis was

obtained with the same enzymatic activity (500 U) corresponding to 100 µg.mL^{-1}, 200 µg.mL^{-1} and 1 mg.mL^{-1} of Sm-PLGV, rPLA$_2$(-5) and rPLA$_2$(+5) respectively (Fig. B.4) after 30 min incubation. Long chain which has a lower activity than rPLA$_2$(+5) and rPLA$_2$(-5), showed the lowest hemolytic power (10%) after the same incubation time.
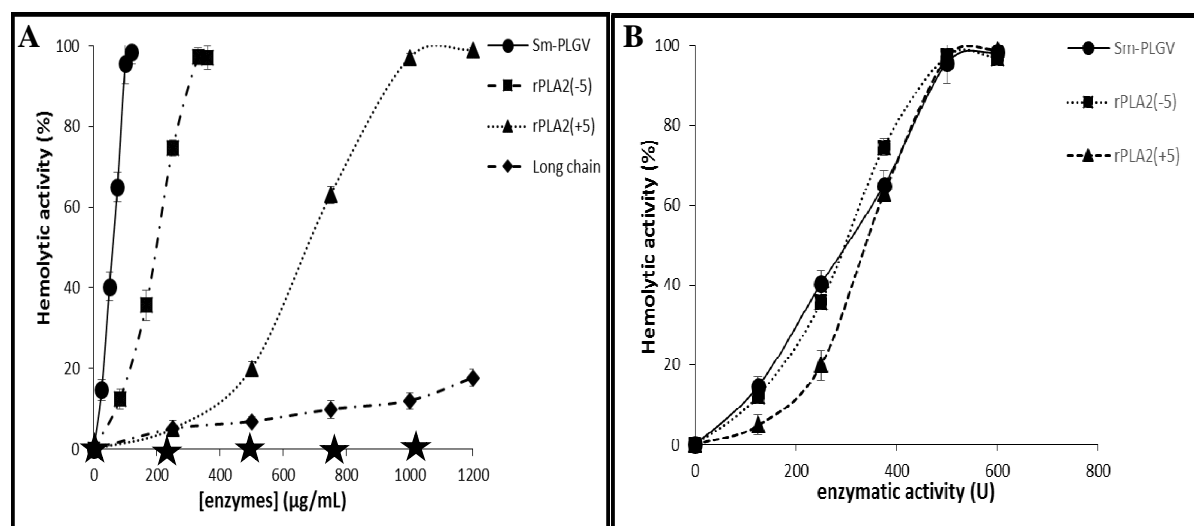

Figure 4: Hemolytic activity of Sm-PLGV, rPLA$_2$(-5), rPLA$_2$(+5) and Long chain. Freshly prepared human erythrocytes were incubated with various enzyme concentrations **(A)** or activity **(B)** of Sm-PLGV, rPLA$_2$(-5), rPLA$_2$(+5) and Long chain, for 30 min at 37 °C. Sm-PLGV was taken as a control. The stars represent the hemolytic activity obtained with all phospholipases inhibited by 1 mM p-bromophenacyl bromide (p-BPB).

In order to confirm the relation between hemolytic power and enzyme activity, Sm-PLGV and recombinants variants were treated with p-bromophenacyl bromide (p-BPB), a specific inhibitor of sPLA$_2$. Fig. A.4 shows that after total inhibition, all enzymes became unable to trigger the hemolytic effect. This result confirms the link between hemolysis and enzyme activity as observed with same snake venom PLA$_2$ such as RVVA-PLA$_2$-I from *Daboia russelli* venom [52].

3.8 Variations of the rPLA$_2$(-5), rPLA$_2$(+5) and Long chain activity with surface pressure: a monolayer study

We studied the activity of rPLA$_2$(-5), rPLA$_2$(+5) and Long chain on phospholipid monolayers at various surface pressures to investigate the possible correlation between the

19

enzyme capacity to penetrate phospholipid layers at high surface pressure and phospholipid hydrolysis in erythrocytes membranes leading to hemolysis. Monolayers of zwitterionic diC_{12}-PE and diC_{12}-PC, and negatively charged PG and PS were tested. In erythrocytes, phosphatidylserine (PS), phosphatidylethanolamine (PE), and phosphatidylinositol (PI) are located mainly in the inner monolayer while phosphatidylcholine (PC) and sphingomyelin (SM) are essentially in the outer monolayer [53].

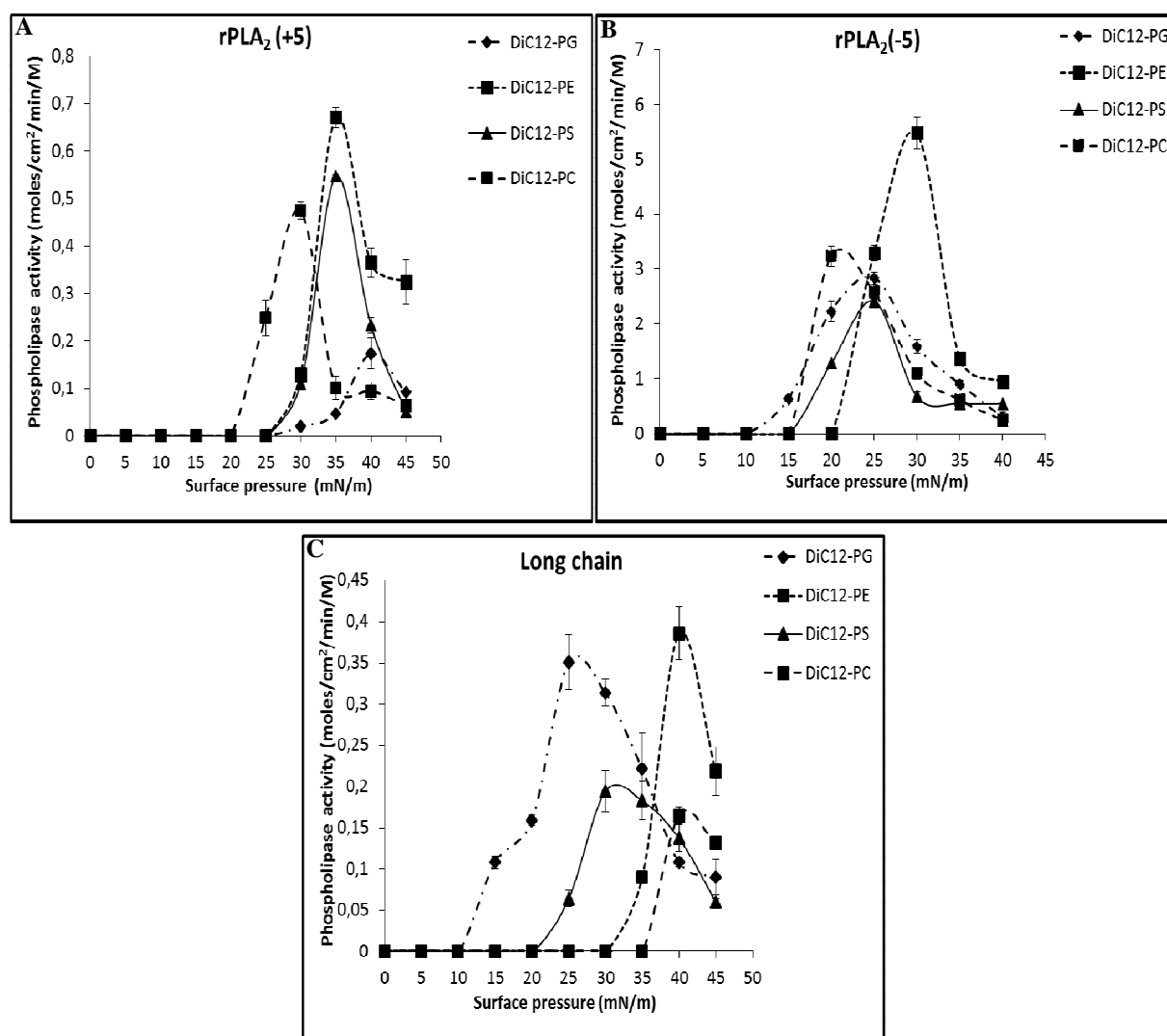As found for Sm-PLVG, all recombinant variants were more active on diC_{12}-PE films than on diC_{12}-PC, PG and PS films.

Figure 5: Variation with surface pressure of **(A)** rPLA$_2$(+5), **(B)** rPLA$_2$(-5) and **(C)** Long chain activity on various medium chain phospholipids (diC_{12}-PC , diC_{12}-PE , PG and PS). Phopsholipase activity is expressed as the number of moles of substrates hydrolyzed by unit time and unit surface of the reaction compartment of the "zero-order". Activity measurements were performed after 10 min of enzymes injection under substrate monomolecular films. The kinetic experiments were recorded as described in Material and methods.

As expected from their respective enzymatic activities on egg PC in bulk, hydrolysis of phospholipid monolayers by $rPLA_2(-5)$ was higher than that of $rPLA_2(+5)$ or Long chain which was the lowest. Remarkably, maximum hydrolysis of phospholipid monalayers by $rPLA_2(-5)$ was shifted towards lower surface pressures compared to $rPLA_2(+5)$ or Long chain. The highest enzymatic activities for both recombinant enzymes were recorded on diC_{12}-PE: 0.67 mol.cm^{-2}.min^{-1}.M^{-1} for $rPLA_2(+5)$ at 30 mN.m^{-1} and 5,48 mol.cm^{-2}.min^{-1}.M^{-1} for $rPLA_2(-5)$ at 35 mN.m^{-1} (Fig. A-B.5). Thus, the hydrolytic activity of $sPLA_2$ is influenced by the chemical nature of phospholipids molecules and their physical state. Despite the activities of Sm-PLVG on diC_{12}-PG and diC_{12}-PS which were very low [31], $rPLA_2(+5)$ and $rPLA_2(-5)$ showed a high rate of hydrolysis of negatively charged head group PG and PS at high surface pressure. This kinetic property of $rPLA_2(+5)$ and $rPLA_2(-5)$ can be correlated to their capacity to attack biological membranes [2]. The low hemolytic activity of Long chain can be related to the low rate of hydrolysis of diC_{12}-PE (0.38 mol.cm^{-2}.min^{-1}.M^{-1}) and PS (0.16 mol.cm^{-2}.min^{-1}.M^{-1}) at high surface pressure (40 mN.m^{-1}) compared to $rPLA_2(+5)$ and $rPLA_2(-5)$. (Fig. 5.C)

3.9 IR-Spectroscopy of Sm-PLVG, $rPLA_2(+5)$, $rPLA_2(-5)$ and Long chain

FTIR spectra of $rPLA_2(+5)$, $rPLA_2(-5)$, Long chain and Sm-PLVG were recorded and the amide I was deconvoluted. In all cases, it displays three major components and several shoulders (Fig. 6). All spectra exhibit the same global shape, vibrational bands and structural components, confirming that all constructs are well folded in the same global secondary structure.
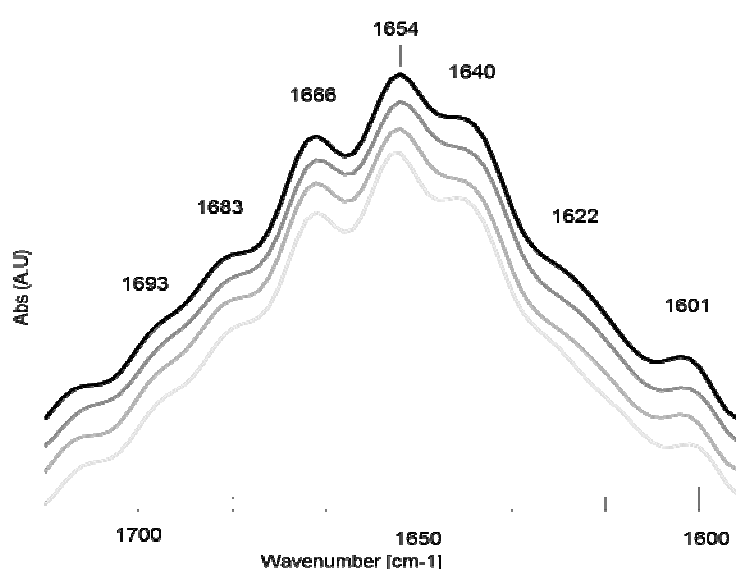
Figure 6: Deconvoluted FTIR absorption spectra of *Scorpio maurus* phospholipases in the Amide I region. From top to bottom: rPLA$_2$(+5) (black), native Sm-PLVG (darker grey), recombinant Long chain (grey) and rPLA$_2$(-5) (lighter grey)

The band at 1666 cm^{-1} can be attributed to the global vibration of β-sheet [54], while the one at 1654 cm^{-1} represents a combination of the vibrations of α-helix and random coil [55], which can exhibit quite the same vibrational bands in IR spectrum recorded in water [56]. The band at 1640 cm^{-1} can be attributed to β-sheet and is related to the shoulder at 1683 cm^{-1} characteristic of rippled β-sheet [55]. The last three shoulders at 1693, 1622 and 1601 cm^{-1} in the spectrum can be attributed to amino acid vibrations whose important contribution to protein spectrum recorded in water is well documented [57]. They might be attributed to arginine involved in salt bridges, tryptophan and tyrosine respectively [57]. Since no vibration at 1672 cm^{-1} was detectable, all arginine residues in the different protein constructs seem to be engaged in salt bridges. The overlay of the deconvoluted FTIR spectra of native Sm-PLVG and rPLA$_2$(-5) shows no remarkable difference, confirming their structural similarity. All observed differences in the deconvoluted FTIR spectra of the variant proteins are summarized in Table 3.

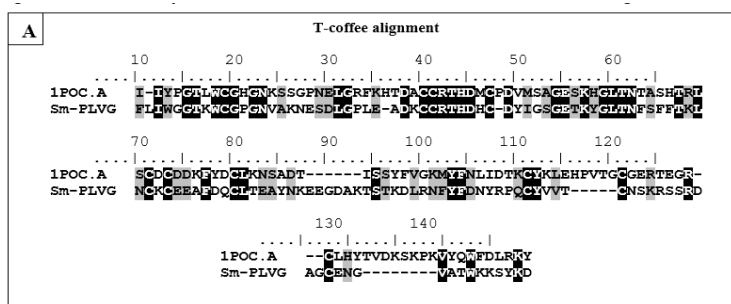**Table 3**: Structural interpretation of deconvoluted FTIR spectra

Protein	Observation in spectrum	Interpretation of observation	Impact on structure/folding	Remarks for model building
rPLA$_2$(+5) Long chain rPLA$_2$(-5)	No signal at 1620 cm^{-1}	No β-sheets of intramolecular aggregation	All three constructs are well folded	The short chain does not build up a large (hydrophobic) interface with the catalytic domain or penetrates deeply in the fold.
rPLA$_2$(+5) Long chain rPLA$_2$(-5)	Same global spectral shape	All three proteins have a very similar secondary structure	The presence or absence of the short chain does not impact on the fold of the catalytic domain	The short chain does not add a domain with high secondary structure content.
rPLA$_2$(+5) Long chain rPLA$_2$(-5)	Clear signal at 1693 cm^{-1} for Arginine involved in salt bridges; no signal at 1672 cm^{-1} corresponding to unbound Arginine	All Arginine residues are similarly involved in salt bridges	The two Arginine present in the penta-peptide insert are also engaged in salt bridges	One or both Arginine might be in contact with the C-terminal Aspartate

rPLA$_2$(-5)	More pronounced β-sheet shoulder at 1640 cm^{-1}	Higher contribution of β-sheet	The short chain adds a β-strand, but only if the penta-peptide insert is deleted	The short chain creates a β-strand after deletion of the penta-peptide insert
rPLA$_2$(-5)	α-helix vibration at 1655 cm^{-1} shifted to higher wavenumber	Overall α-helices are less H-bonded or less exposed to solvent	Deletion of the penta-peptide insert reorganizes the chain to cover α-helices	Most probable candidate is the short chain as it has been reorganized (see above)
rPLA$_2$(-5)	Tyrosine vibration at 1600 cm^{-1} shifted to lower wavenumber	Overall Tyrosine content is more exposed to solvent or in polar contacts	Deletion of the penta-peptide uncovers a Tyrosine or creates a polar interaction with a Tyrosine The reorganized short chain contains a Tyrosine which might be the cause	

3.10 Molecular modelling of rPLA$_2$(+5), rPLA$_2$(-5) and Long chain

To better understand our experimental data and the role of the short chain at a molecular level, we constructed structural models of rPLA$_2$(+5), rPLA$_2$(-5) and Long chain. Long chain shares a sequence identity of 39 % and the same Cysteine pattern with the honeybee venom PLA$_2$ (pdb code: 1poc; further on called hbPLA$_2$). A reasonable model of Long chain was directly obtained from the automated Swissmodel server. In this model, the fold of three main helices A, B and C observed in hbPLA$_2$ is maintained, even though an additional loop is inserted between helices B and C. Also, the two stranded β-sheet between helices A and B is conserved, as well as all residues of the Ca^{2+} binding site and the key catalytic residues His34, Asp/Glu63 and Tyr92. The C-terminal extension after the disulfide bridge C60-C100 is truncated after Ser107 in Long chain and is 5 to 10 residues shorter in rPLA$_2$(+5) and rPLA$_2$(-5) than in hbPLA$_2$. It has no significant identity with other published PLA$_2$ structures. The prediction of its fold is therefore not obvious. A BLAST search of the last 29 residues behind Cys100 against the pdb database results in a best hit with 69% identity only for the final half of the sequence, aligned to a region inside the yeast Copper-Zinc-Superoxide dismutase (1SDY) which is folded as a loop followed by a C-terminal β-strand.

23

Remarkably also the C-terminus in hbPLA$_2$ forms a loop structure followed by a β-strand and some of the residues in this section, including Trp123 which occupies a hydrophobic pocket in hbPLA$_2$, are conserved in Sm-PLVG (Fig. A.7). It seems therefore reasonable to model a similar conformation of the short chain taking the bee-venom as reference. Another resemblance with hbPLA$_2$ is the presence of two arginine residues at the extremity of the long loop proceeding the C-terminal β-strand in hbPLA$_2$, as it can be found in the scissile penta-peptide in rPLA$_2$(+5). Supposing a structural homology, the latter might be similarly exposed at the extremity of a similar but shorter loop in rPLA$_2$(+5). Essential information for the modeling of the short chain could be obtained from the deconvoluted FTIR spectra of the variants, whose results and conclusions are summarized in Table 2. Interestingly, a higher β-strand content is only present in rPLA$_2$(-5) suggesting that an interaction of the short chain with the scissile penta-peptide in rPLA$_2$(+5) disorders its β-strand structure. In hbPLA$_2$ the C-terminus is a Tyrosine buried in a hydrophobic pocket. It is replaced by Asp129 in Sm-PLVG, who might form salt bridges with either the Arginine residues in the scissile penta-peptide present in rPLA$_2$(+5) or with an Arginine occupying the same location in Sm-PLVG as the hydrophobic interaction in hbPLA$_2$. The proposed models of all three constructs have been checked for reasonable bond geometries and contain no outliers in the Ramachandran plot (Fig. B-C. 7).
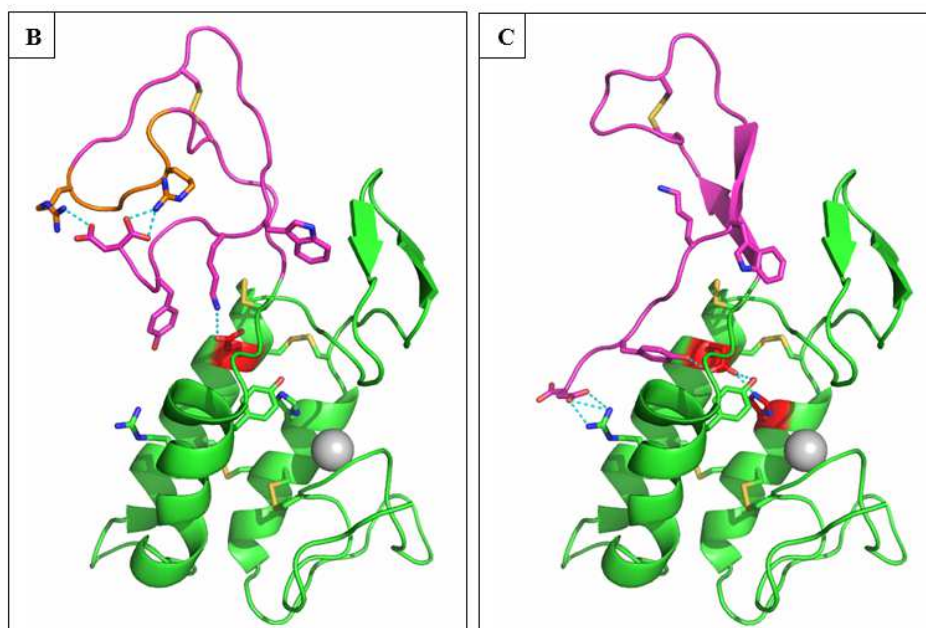
Figure 7: 3D modeling of *Scorpio maurus* phospholipase. (**A**) T-coffee alignment of the sequence of Sm-PLVG with bee venom PLA_2 (pdb code: 1poc.A) which served as the structural basis for modeling. 3D models of $rPLA_2(+5)$ (**B**) and $rPLA_2(-5)$ (**C**) with side chain interactions are shown in panels **B** and **C**, respectively. The C-terminal extensions after Cys100 are colored in magenta. The catalytic diade Glu63/His34 is colored in red and the pentapeptide insert of $rPLA_2(+5)$ in orange. The Additional β-sheet in $rPLA_2(-5)$ is colored in magenta. H-bonds of the active site diade, arginine residues in the inserted pentapeptide and c-terminal Asp residue are shown in cyan. The Ca^{2+} ion is shown as a grey sphere.

Clues for the interpretation of the experimental data can be found by analyzing the constructed models. An important difference between $hbPLA_2$ and Sm-PLVG is the replacement of the Asp in the catalytic Asp/His pair by a more flexible Glu63 in the latter. The observed variation in activity of the constructs might be related to the intensity of the Glu63/His34 interaction in the active site. If this interaction is disturbed, the pKa of the catalytic His34 will change, impacting the stabilization of the transition state, i.e. the enzymes activity, and also indirectly via a coordinated water molecule the capture of the Ca^{2+} ion in the active site. The truncation of the short chain in the Long chain construct deletes a stabilizing residue in the proximity of the Glu63. In $hbPLA_2$, a leucine residue in the C-terminal part creates a hydrophobic barrier to the surface just behind this catalytic Asp, favoring its interaction with the catalytic His. In Long chain, this residue is absent, what creates an access to the solvent permitting the more flexible Glu63 to disengage its interaction with His34 and to reorient to the polar surface, largely reducing its activity. The same situation can be observed in the $rPLA_2(+5)$ model, in which additionally a positively charged residue (here: Lys124) of the short chain might penetrate into this access to stabilize Glu63 in this non-

productive orientation. After deletion of the penta-peptide insertion, the short chain is reoriented as a β-strand, what ends this non-productive interaction. It can introduce Tyr127 in the access behind Glu63, what not only recreates a barrier to the surface, but also might stabilize the interaction of Glu63 with His34 via an H-bond with his phenolic hydroxyl function. A similar stabilization of the catalytic acid by two tyrosine residues can be observed in group I and II PLA_2, but not in $hbPLA_2$.

The overall electrostatic charge distribution on the surface of the models reveals a mostly hydrophobic section around the binding pockets of the acyl chains, but a net negative potential in the head-group binding pocket of all our constructs what might favor the interaction with zwitterionic phospholipids containing a positively charged amine or choline group (Fig. 8). An additional positively charged patch at the vicinity of the active site is countered by a negative patch on the opposite site of the protein. The presence of two opposed charges at each side of the molecule generate a dipole moment parallel to the orientation of the active site access what might help to orient the enzymes active site correctly towards the negative charges of the phospholipid layer. The reduction of the calculated dipole moment from 452 D in $rPLA_2(-5)$ and 374 D in Long chain to 317 D in $rPLA_2(+5)$ due to the positive charge of the short chain and the pentapeptide, seems to influence the overall surface pressure/activity optimum since we observe a shift from low to high surface pressures in our hydrolysis experiments with phospholipid films.
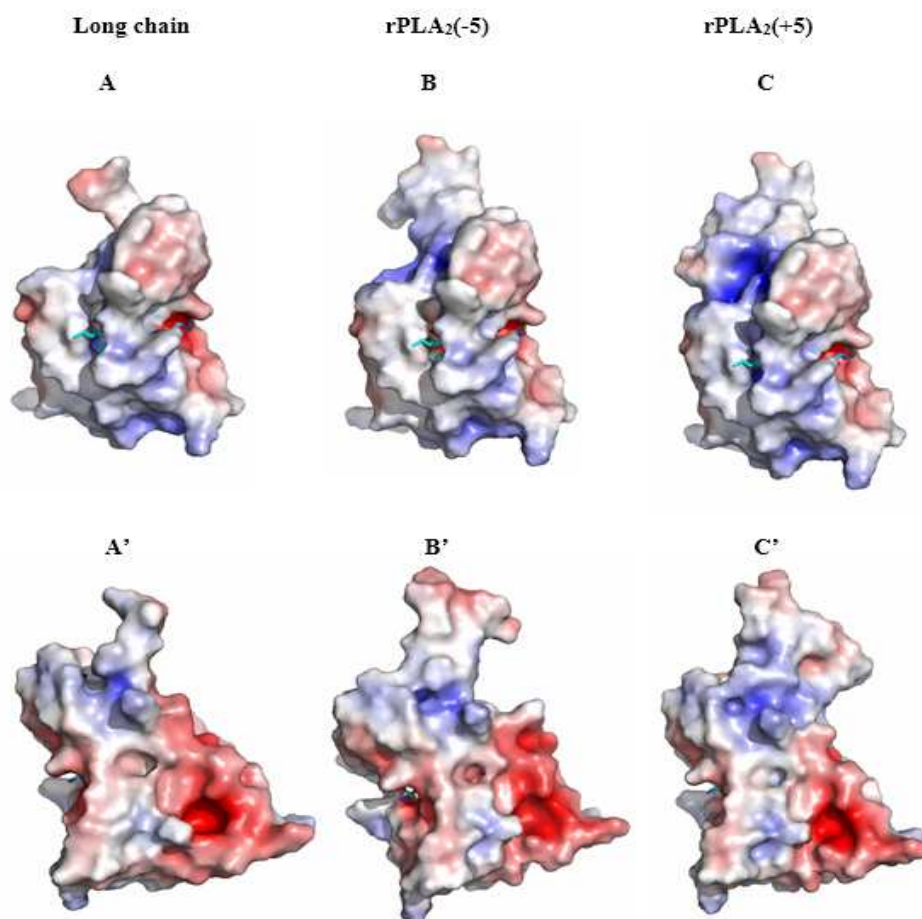
Figure 8: 3D models with surface potential of Long chain (A, A'), $PLA_2(-5)$ (B, B') and $PLA_2(+5)$ (C, C'). Surface potentials were calculated with APBS. Positive potential is colored blue and negative potential red. The phospholipid substrate from the bee venom structure 1poc.pdb has been overlaid with the structure and is visible in cyan (stick model). In the upper panels A, B and C, the negatively charged Phosphate binding pocket is on the right side while the mostly hydrophobic acyl chain-binding cleft is on the left. The lower panels A', B' and C' show views of the same models after a 180-degree perpendicular rotation.

4. Discussion

A phospholipase A₂ named Sm-PLVG was purified and characterized directly from the venom glands of Tunisian scorpion *Scorpio maurus* [31]. We cloned its gene and we produced three recombinant forms of Sm-PLVG in *Escherichia coli* to further study the structure-function relationships of this enzyme.

The gene that encodes full length Sm-PLGV is transcribed into a single mRNA, coding for the long and the short chain, separated by a penta-peptide Lys-Arg-Ser-Ser-Arg, which is cleaved during maturation. The same maturation procedure has been observed in other scorpion venom PLA₂ such as IpTxi [16] and phospholipin [30] from *Pandinus imperator* or MtPLA₂ from *Mesobuthus tumulus* [28]. The mRNA sequence that encodes Sm-PLGV is composed of 387 nucleotides (including the stop codon), starting at residue Phe1 and ending at residue Asp129, just before the stop codon. There is no N-terminal pro-peptide as observed in some other PLA₂. A homology search indicates that Sm-PLGV has a high sequence homology of 84% with *Pandinus imperator* PLA₂ sequence Phospholipin [30] and 78% homology with Phaiodactylipin from *Anuroctonus phaiodactylus* venom [17], but no significant sequence identity with the well-studied group I and II PLA₂ (Fig. 9).

```
                 *                        ** ##  *
Sm    FLIWGGTKWCGPGNVAKNESDLGPLE-ADKCCRTHDHC-DYIGSGETKYG 48
Ph    FLMWECTKWCGPGNNAKCESDLGPLE-ADKCCRTHDHC-DYIASGETKYG 48
Ix    --TMWGTKWCGSGNEATDISELGYWSNLDSCCRTHDHC-DNIPSGQTKYG 47
Am    -IIYPGTLWCGHGNKSSGPNELGRFKHTDACCRTHDMCPDVMSAGESKHG 49
Mt    --TMWGTKWCGSGNEAINYTDLGYFSNLDSCCRTHDHC-DSIPAGETKYG 47
Hl    --TVWGTKWCGSGNEATSGIDLGYFKNLDSCCRTHDHC-DNIPAGETKYG 47
Ap    FLIVSGTKWCGNNNIAANYSDLGFLE-ADKCCRDHDHC-DHIASGETKYG 48

             *  *#        *
Sm    LTNFSFFTKLNCKCEEAFDQCLTEAYNKEEGD--AKTSTKDLRNFYFDNY 96
Ph    ITNYAFFTKLNCKCEEAFDRCLTEAYNKEEKES-AKSSTKRLQNFYFGTY 97
Ix    LTNEGKYTMMNCKCETAFEQCLRNVTGGMEGP-----AAGFVRKTYFDLY 92
Am    LTNTASHTRLSCDCDDKFYDCLKNSADTISSY--------FVGKMYFNLI 91
Mt    LTNEGKYTMMNCKCESAFEKCLRDVRGILEGK-----AAAAVRKTYFDLY 92
Hl    LTNEGIYTMMNCKCESVFKQCLKDVTGVFEGP-----AAAAVRKIYFDLY 92
Ap    LENKGLFTILNCDCDEAFDHCLKEISNNVTTDIRQKGGAENVWRFYFQ-W 97

          *       *              *
Sm    RPQCYVVTCNS-KRSSRDAG-CENGVATWK--KSYKD-------- 129
Ph    SPECYVVTCNS-KRSGRDAG-CENGVATWK--KSYKD-------- 130
Ix    GNGCYNVQCPSQRRLARSEE-CPDGVATYTGEAGYGAWAINKLNG 136
Am    DTKCYKLEHPVTGCGERTEGRCLHYTVDKSKPKVYQWFDLRKY-- 134
Mt    GNGCFNVKCPSGARSARSEE-CTNGMATYTGETGYGAWAINKLNG 136
Hl    GNGCYSVQCPAGGRSARTGG-CPNGVATYTGETGYGAWLLNKANG 136
Ap    NANCYRLYCKD-EKSARDEA-CTNQYAVVK--KNFTVQ------- 131
```

Figure 9: Sm-PLGV amino acid sequence alignment with other PLA₂ from scorpion and bee venoms. *Sm: Scorpio maurus* PLA₂, Ph: phospholipin from *Pandinus imperator*, Ix: Imperatoxin from *Pandinus imperator*, Am: *Apis mellifera*, Mt: *Mesobuthus tumulus*, Hl: *Heterometrus loaticus*, Ap: *Anuroctonus phaiodactylis*.
* Represents conserved cysteine residues, **#** indicates the main catalytic residues, Residues showed in grey box indicate the calcium-binding loop. Residues underlined indicate putative N-glycosylation sites. The alignment of the short chain region is framed.

In the Long chain of processed Sm-PLGV, the catalytic Histidine at position 34 is conserved and preceded by a DXCCRX motif as in other group III PLA$_2$. Also the Ca^{2+} binding loop motif, GTXWCGXG and all eight cysteines which are essential features in group III PLA$_2$ are conserved (Fig. 9). Obviously, the long chain is bearing the principal features of the phospholipase active site in scorpion venom PLA$_2$.

Otherwise in the rPLA$_2$(+5) or rPLA$_2$(-5), the C-terminal part of the sequence which is processed to become the short chain has low sequence identity inside group III PLA$_2$. Different subgroups with similar C-terminal extensions can be found in group III PLA$_2$, and Sm-PLVG is part of a group including scorpion venom PLA$_2$ from *P. imperator* (phospholipin; ID: P0DKU2.1), *Hadrurus spadix* (PLA$_2$; ID: JAV47952.1) or *Hemiscorpius lepturus* (HLlipin-2; ID: API81337.1).

Phospholipase activity was tested at temperatures ranging from 25 to 60°C using egg-PC as substrate (Fig. A.3). In contrast to many venom PLA$_2$ produced in *E. coli*, such as rPLA$_2$ from *Mesobuthus tumulus* scorpion venom [49], Honey bee [58], snake venoms *Bothrops diporus* [59] and *Lapemis hardwickii* [60] whose maximum activity on phospholipids is at 25°C, the maximum activity of Sm-PLGV is found at 50°C [31]. All the variants show the same temperature optimum but are less active. The most active recombinant form rPLA$_2$(-5) is 3.6 fold less active (1500 U/mg) than Sm-PLGV (5500 U/mg) what might be related to the covalent connection of the long and short chains. The presence of the penta-peptide KRSSR in rPLA$_2$(+5) leads to a 3.3 fold decrease in enzyme activity (450 U/mg). Finally, enzyme activity further dropped nearly ten times in the absence of the short chain and overall enzyme stability was reduced.

Thermostability data of our recombinant enzymes showed that rPLA$_2$(+5) and rPLA$_2$(-5) retained 85% of their maximal activity after incubation at 37°C. At temperatures over 50°C, the activity decreased dramatically and the enzymes lost all their activity over 65°C. Thermal inactivation of rPLA$_2$(-5) and rPLA$_2$(+5) follow the same profile as Sm-PLGV. These data point to a two-step unfolding of the PLA2 chains, where the short chain unfolds first to give an intermediate fold at 45°C maintaining the catalytic domain mostly intact and then further unfolds at higher temperatures. If the short chain is absent, like in the Long chain variant, stability of the remaining catalytic domain degrades much faster to this intermediate. These results are not completely in agreement with our data on maximum activity of the variants at 50°C. It is likely that under these test conditions the presence of substrate has a thermo-protective effect, as proposed by Verger and Cherif [61, 62]. In the absence of

substrate, when the enzyme is in the aqueous phase, the enzymes are rapidly inactivated at higher temperatures.

Besides its influence on unfolding, the short chain has a large impact on the activity of the catalytic domain. Even though the Long chain variant contains the active site and the calcium binding loop, its enzymatic activity is very low (AS= 50 U/mg) compared to rPLA$_2$(+5) and rPLA$_2$(-5). We constructed molecular models of all these variants to understand the influence of the short chain on enzyme activity. The available FTIR data gave us additional hints for the interaction of the short chain with the principle catalytic domain. FTIR data and 3D modeling suggest that a structural rearrangement of the short chain after deletion of the penta-peptide may be responsible for the establishment of a productive Glu63/His34 interaction. This might explain the observed changes of catalytic activity via a change of pKa of His34 and can impact on the affinity of the Calcium site via a bridging water or substrate molecule. An additional inhibitory effect of the released penta-peptide on the active site as has been postulated in the case of MtPLA$_2$ [28] is still possible but cannot be confirmed by our approach.

Since native Sm-PLGV showed direct hemolytic activity, we tested if its recombinants forms conserve this activity despite their difference in specific activity (Fig. 4). ValdezCruz and al., [17] showed that phaiodactylipin from *Anuroctonus phaiodactylus* and Iptxi from *Pandinus imperator* causes direct hemolytic action on human erythrocytes after 10 min of incubation. rPLA$_2$(-5) and rPLA$_2$(+5) lysed all erythtrocytes after 30 min at 200 µg.mL^{-1} and 1 mg.mL^{-1} respectively but Long chain was tenfold less active (10 % lysis) after the same incubation time in accordance with catalytic activity data. Our results showed the dependence of the hemolytic on enzymatic activity (Fig. A. 5). We have no evidence for a distinct interaction of Sm-PLVG short chain with biological membranes as postulated previously.

It is well documented that the different venom PLA$_2$ can display dramatically different affinities for biomembranes, composed of different phospholipid polar head groups and fatty acyl chains, resulting in their differential membrane damaging activity. The differences in overall net charge in a venom PLA$_2$ molecule may attribute to differential binding and subsequent hydrolysis of phospholipids of a particular membrane [52].

We showed that rPLA$_2$(+5) and rPLA$_2$(-5) are able to hydrolyze phospholipid monolayers at high surface pressure like Sm-PLGV, which well correlates with their ability to hydrolyze phospholipids in erythrocyte cell membranes, as previously shown with other phospholipases A$_2$ like the sPLA$_2$ from venom *Naja naja* PLA$_2$ [63]. The highest enzyme

activities on diC_{12}-PE and diC_{12}-PC were recorded at surface pressures of 30 and 35 mN.m^{-1} for $rPLA_2$(+5) (Fig. A.5) and PLA_2(-5) (Fig. B.5), respectively. As observed with Sm-PLVG, $rPLA_2$(+5) and $rPLA_2$(-5), activities on these zwitterionic phospholipid films were higher than those measured on negatively-charged phospholipid films (PG and PS). This may result from the negative net charge of the head-group binding pocket in the enzyme. The activity of Sm-PLVG on negatively-charged PG and PS was previously found to be very low [31]. Nevertheless, $rPLA_2$(+5) and $rPLA_2$(-5) showed a high rate of hydrolysis of PG and PS at high surface pressure. This behavior is similar to PLA_2 from *vipera berus* which hydrolysis negatively charged head group at high surface pressure more than zwitterionic phospholipids[64]. These differences in hydrolysis rates can be correlated to difference in interfacial binding to phospholipids that depend on their polar head and physical state.

Conclusion

We cloned the gene coding the PLA$_2$ from venom glands of Tunisian scorpion *Scorpio maurus* and we produced three recombinant forms of this enzyme in *Escherichia coli* to further study its structure-function relationships. Recombinants constructs are rPLA$_2$(+5) which contains the penta-peptide, rPLA$_2$(-5) without penta-peptide and Long chain without short chain. A comparative study between biochemical and interfacial properties of the native Sm-PLGV and recombinant phospholipases A$_2$ showed the importance of the short chain in the stability and enzymatic activity.

FTIR-based 3D modeling of three recombinant constructs undergo the difference of the enzymatic activities of these PLA$_2$. After deletion of the penta-peptide, a structural rearrangement of the short chain allows it to interact with the principle catalytic site, which can explain the decrease of long chain activity. Overall, the results presented here bring new informations on the scorpion PLA$_2$ properties.

Acknowledgments

References

[1] I. Kudo, M. Murakami, Phospholipase A2 enzymes, Prostaglandins & other lipid mediators, 68-69 (2002) 3-58.

[2] H.M. Verheij, A.J. Slotboom, G.H. de Haas, Structure and function of phospholipase A2, Reviews of physiology, biochemistry and pharmacology, 91 (1981) 91-203.

[3] J.J. Seilhamer, T.L. Randall, M. Yamanaka, L.K. Johnson, Pancreatic phospholipase A2: isolation of the human gene and cDNAs from porcine pancreas and human lung, DNA, 5 (1986) 519-527.

[4] E.A. Dennis, The growing phospholipase A2 superfamily of signal transduction enzymes, Trends in biochemical sciences, 22 (1997) 1-2.

[5] D.A. Six, E.A. Dennis, The expanding superfamily of phospholipase A(2) enzymes: classification and characterization, Biochimica et biophysica acta, 1488 (2000) 1-19.

[6] M. Rouault, J.G. Bollinger, M. Lazdunski, M.H. Gelb, G. Lambeau, Novel mammalian group XII secreted phospholipase A2 lacking enzymatic activity, Biochemistry, 42 (2003) 11494-11503.

[7] R.H. Schaloske, E.A. Dennis, The phospholipase A2 superfamily and its group numbering system, Biochimica et biophysica acta, 1761 (2006) 1246-1259.

[8] R.M. Kini, Excitement ahead: structure, function and mechanism of snake venom phospholipase A2 enzymes, Toxicon : official journal of the International Society on Toxinology, 42 (2003) 827-840.

[9] D. Fenard, G. Lambeau, E. Valentin, J.C. Lefebvre, M. Lazdunski, A. Doglio, Secreted phospholipases A(2), a new class of HIV inhibitors that block virus entry into host cells, The Journal of clinical investigation, 104 (1999) 611-618.

[10] P.G. Roberto, S. Kashima, S. Marcussi, J.O. Pereira, S. Astolfi-Filho, A. Nomizo, J.R. Giglio, M.R. Fontes, A.M. Soares, S.C. Franca, Cloning and identification of a complete cDNA coding for a bactericidal and antitumoral acidic phospholipase A2 from Bothrops jararacussu venom, The protein journal, 23 (2004) 273-285.

[11] A. Bazaa, J. Luis, N. Srairi-Abid, O. Kallech-Ziri, R. Kessentini-Zouari, C. Defilles, J.C. Lissitzky, M. El Ayeb, N. Marrakchi, MVL-PLA2, a phospholipase A2 from Macrovipera lebetina transmediterranea venom, inhibits tumor cells adhesion and migration, Matrix biology : journal of the International Society for Matrix Biology, 28 (2009) 188-193.

[12] R. Kessentini-Zouari, J. Jebali, S. Taboubi, N. Srairi-Abid, M. Morjen, O. Kallech-Ziri, S. Bezzine, J. Marvaldi, M. El Ayeb, N. Marrakchi, J. Luis, CC-PLA2-1 and CC-PLA2-2, two Cerastes cerastes venom-derived phospholipases A2, inhibit angiogenesis both in vitro and in vivo, Laboratory investigation; a journal of technical methods and pathology, 90 (2010) 510-519.

[13] K. Kuchler, M. Gmachl, M.J. Sippl, G. Kreil, Analysis of the cDNA for phospholipase A2 from honeybee venom glands. The deduced amino acid sequence reveals homology to the corresponding vertebrate enzymes, European journal of biochemistry, 184 (1989) 249-254.

[14] Y. Ryu, Y. Oh, J. Yoon, W. Cho, K. Baek, Molecular characterization of a gene encoding the Drosophila melanogaster phospholipase A2, Biochimica et biophysica acta, 1628 (2003) 206-210.

[15] D.L. Scott, Z. Otwinowski, M.H. Gelb, P.B. Sigler, Crystal structure of bee-venom phospholipase A2 in a complex with a transition-state analogue, Science, 250 (1990) 1563-1566.

[16] F.Z. Zamudio, R. Conde, C. Arevalo, B. Becerril, B.M. Martin, H.H. Valdivia, L.D. Possani, The mechanism of inhibition of ryanodine receptor channels by imperatoxin I, a heterodimeric protein from the scorpion Pandinus imperator, The Journal of biological chemistry, 272 (1997) 11886-11894.

[17] N.A. Valdez-Cruz, C.V. Batista, L.D. Possani, Phaiodactylipin, a glycosylated heterodimeric phospholipase A from the venom of the scorpion Anuroctonus phaiodactylus, European journal of biochemistry, 271 (2004) 1453-1464.

[18] P. Incamnoi, R. Patramanon, S. Thammasirirak, A. Chaveerach, N. Uawonggul, S. Sukprasert, P. Rungsa, J. Daduang, S. Daduang, Heteromtoxin (HmTx), a novel heterodimeric phospholipase A(2) from Heterometrus laoticus scorpion venom, Toxicon : official journal of the International Society on Toxinology, 61 (2013) 62-71.

[19] G. Hariprasad, B. Singh, U. Das, A.S. Ethayathulla, P. Kaur, T.P. Singh, A. Srinivasan, Cloning, sequence analysis and homology modeling of a novel phospholipase A2 from Heterometrus fulvipes (Indian black scorpion), DNA sequence : the journal of DNA sequencing and mapping, 18 (2007) 242-246.

[20] F. Gomez, A. Vandermeers, M.C. Vandermeers-Piret, R. Herzog, J. Rathe, M. Stievenart, J. Winand, J. Christophe, Purification and characterization of five variants of phospholipase A2 and complete primary structure of the main phospholipase A2 variant in Heloderma suspectum (Gila monster) venom, European journal of biochemistry, 186 (1989) 23-33.

[21] E. Valentin, F. Ghomashchi, M.H. Gelb, M. Lazdunski, G. Lambeau, Novel human secreted phospholipase A(2) with homology to the group III bee venom enzyme, The Journal of biological chemistry, 275 (2000) 7492-7496.

[22] E. Valentin, G. Lambeau, Increasing molecular diversity of secreted phospholipases A(2) and their receptors and binding proteins, Biochimica et biophysica acta, 1488 (2000) 59-70.

[23] L. Touqui, M. Alaoui-El-Azher, Mammalian secreted phospholipases A2 and their pathophysiological significance in inflammatory diseases, Current molecular medicine, 1 (2001) 739-754.

[24] M.T. Murakami, R.K. Arni, A structure based model for liposome disruption and the role of catalytic activity in myotoxic phospholipase A2s, Toxicon : official journal of the International Society on Toxinology, 42 (2003) 903-913.

[25] T.R. Costa, D.L. Menaldo, C.Z. Oliveira, N.A. Santos-Filho, S.S. Teixeira, A. Nomizo, A.L. Fuly, M.C. Monteiro, B.M. de Souza, M.S. Palma, R.G. Stabeli, S.V. Sampaio, A.M. Soares, Myotoxic phospholipases A(2) isolated from Bothrops brazili snake venom and synthetic peptides derived from their C-terminal region: cytotoxic effect on microorganism and tumor cells, Peptides, 29 (2008) 1645-1656.

[26] M. Murakami, S. Masuda, S. Shimbara, Y. Ishikawa, T. Ishii, I. Kudo, Cellular distribution, post-translational modification, and tumorigenic potential of human group III secreted phospholipase A(2), The Journal of biological chemistry, 280 (2005) 24987-24998.

[27] I. Jridi, I. Catacchio, H. Majdoub, D. Shahbazeddah, M. El Ayeb, M.A. Frassanito, D. Ribatti, A. Vacca, L. Borchani, Hemilipin, a novel Hemiscorpius lepturus venom heterodimeric phospholipase A2, which inhibits angiogenesis in vitro and in vivo, Toxicon : official journal of the International Society on Toxinology, 105 (2015) 34-44.

[28] G. Hariprasad, M. Kumar, A. Srinivasan, P. Kaur, T.P. Singh, O. Jithesh, Structural analysis of a group III Glu62-phospholipase A2 from the scorpion, Mesobuthus tamulus: Targeting and reversible inhibition by native peptides, International journal of biological macromolecules, 48 (2011) 423-431.

[29] M. Ramanaiah, P.R. Parthasarathy, B. Venkaiah, Purification and properties of phospholipase A2 from the venom of scorpion, (Heterometrus fulvipes), Biochemistry international, 20 (1990) 931-940.

[30] R. Conde, F.Z. Zamudio, B. Becerril, L.D. Possani, Phospholipin, a novel heterodimeric phospholipase A2 from Pandinus imperator scp6pion venom, FEBS letters, 460 (1999) 447-450.

[31] H. Louati, N. Krayem, A. Fendri, I. Aissa, M. Sellami, S. Bezzine, Y. Gargouri, A thermoactive secreted phospholipase A(2) purified from the venom glands of Scorpio maurus: relation between the kinetic properties and the hemolytic activity, Toxicon : official journal of the International Society on Toxinology, 72 (2013) 133-142.

[32] G. Hariprasad, A. Srinivasan, R. Singh, Structural and phylogenetic basis for the classification of group III phospholipase A2, Journal of molecular modeling, 19 (2013) 3779-3791.

[33] M.A. Abdel-Rahman, M.A. Omran, I.M. Abdel-Nabi, O.A. Nassier, B.J. Schemerhorn, Neurotoxic and cytotoxic effects of venom from different populations of the Egyptian Scorpio maurus palmatus, Toxicon : official journal of the International Society on Toxinology, 55 (2010) 298-306.

[34] M.A. Abdel-Rahman, M.A. Omran, I.M. Abdel-Nabi, H. Ueda, A. McVean, Intraspecific variation in the Egyptian scorpion Scorpio maurus palmatus venom collected from different biotopes, Toxicon : official journal of the International Society on Toxinology, 53 (2009) 349-359.

[35] K.M. Bhat, I.G. Sumner, B.N. Perry, M.E. Collins, R.W. Pickersgill, P.W. Goodenough, A novel method for the purification of porcine phospholipase A2 expressed in E. coli, Biochemical and biophysical research communications, 176 (1991) 371-377.

[36] A. Karray, S. Amara, F. Carriere, Y. Gargouri, S. Bezzine, Renaturation and one step purification of the chicken GIIA secreted phospholipase A2 from inclusion bodies, International journal of biological macromolecules, 67 (2014) 85-90.

[37] F. Pattus, A.J. Slotboom, G.H. de Haas, Regulation of phospholipase A2 activity by the lipid-water interface: a monolayer approach, Biochemistry, 18 (1979) 2691-2697.

[38] Y. Gargouri, H. Moreau, G. Pieroni, R. Verger, Human gastric lipase: a sulfhydryl enzyme, The Journal of biological chemistry, 263 (1988) 2159-2162.

[39] M.M. Bradford, A rapid and sensitive method for the quantitation of microgram quantities of protein utilizing the principle of protein-dye binding, Analytical biochemistry, 72 (1976) 248-254.

[40] M. Biasini, S. Bienert, A. Waterhouse, K. Arnold, G. Studer, T. Schmidt, F. Kiefer, T. Gallo Cassarino, M. Bertoni, L. Bordoli, T. Schwede, SWISS-MODEL: modelling protein tertiary and quaternary structure using evolutionary information, Nucleic acids research, 42 (2014) W252-258.

[41] P. Emsley, B. Lohkamp, W.G. Scott, K. Cowtan, Features and development of Coot, Acta crystallographica. Section D, Biological crystallography, 66 (2010) 486-501.

[42] M.D. Winn, C.C. Ballard, K.D. Cowtan, E.J. Dodson, P. Emsley, P.R. Evans, R.M. Keegan, E.B. Krissinel, A.G. Leslie, A. McCoy, S.J. McNicholas, G.N. Murshudov, N.S. Pannu, E.A. Potterton, H.R. Powell, R.J. Read,

A. Vagin, K.S. Wilson, Overview of the CCP4 suite and current developments, Acta crystallographica. Section D, Biological crystallography, 67 (2011) 235-242.

[43] G.N. Murshudov, P. Skubak, A.A. Lebedev, N.S. Pannu, R.A. Steiner, R.A. Nicholls, M.D. Winn, F. Long, A.A. Vagin, REFMAC5 for the refinement of macromolecular crystal structures, Acta crystallographica. Section D, Biological crystallography, 67 (2011) 355-367.

[44] A. Roy, A. Kucukural, Y. Zhang, I-TASSER: a unified platform for automated protein structure and function prediction, Nature protocols, 5 (2010) 725-738.

[45] D. Xu, Y. Zhang, Improving the physical realism and structural accuracy of protein models by a two-step atomic-level energy minimization, Biophysical journal, 101 (2011) 2525-2534.

[46] L. Schrödinger, The PyMOL molecular graphics system, version 1.7. 6.6, in, 2015.

[47] N.A. Baker, D. Sept, S. Joseph, M.J. Holst, J.A. McCammon, Electrostatics of nanosystems: application to microtubules and the ribosome, Proceedings of the National Academy of Sciences of the United States of America, 98 (2001) 10037-10041.

[48] E.F. Pettersen, T.D. Goddard, C.C. Huang, G.S. Couch, D.M. Greenblatt, E.C. Meng, T.E. Ferrin, UCSF Chimera--a visualization system for exploratory research and analysis, Journal of computational chemistry, 25 (2004) 1605-1612.

[49] G. Hariprasad, K. Saravanan, S.B. Singh, U. Das, S. Sharma, P. Kaur, T.P. Singh, A. Srinivasan, Group III PLA2 from the scorpion, Mesobuthus tamulus: cloning and recombinant expression in E. coli, Electronic Journal of Biotechnology, 12 (2009) 6-7.

[50] D.L. Scott, S.P. White, Z. Otwinowski, W. Yuan, M.H. Gelb, P.B. Sigler, Interfacial catalysis: the mechanism of phospholipase A2, Science, 250 (1990) 1541-1546.

[51] D. Bairam, I. Aissa, H. Louati, H. Othman, Z. Abdelkafi-Koubaa, N. Krayem, M. El Ayeb, N. Srairi-Abid, N. Marrakchi, Y. Gargouri, Biochemical and monolayer characterization of Tunisian snake venom phospholipases, International journal of biological macromolecules, 89 (2016) 640-646.

[52] D. Saikia, N.K. Bordoloi, P. Chattopadhyay, S. Choklingam, S.S. Ghosh, A.K. Mukherjee, Differential mode of attack on membrane phospholipids by an acidic phospholipase A(2) (RVVA-PLA(2)-I) from Daboia russelli venom, Biochimica et biophysica acta, 1818 (2012) 3149-3157.

[53] P.F. Devaux, Static and dynamic lipid asymmetry in cell membranes, Biochemistry, 30 (1991) 1163-1173.

[54] H. Susi, D.M. Byler, Fourier transform infrared study of proteins with parallel beta-chains, Archives of biochemistry and biophysics, 258 (1987) 465-469.

[55] E. Goormaghtigh, V. Cabiaux, J.M. Ruysschaert, Determination of soluble and membrane protein structure by Fourier transform infrared spectroscopy. III. Secondary structures, Sub-cellular biochemistry, 23 (1994) 405-450.

[56] A. Barth, Infrared spectroscopy of proteins, Biochimica et biophysica acta, 1767 (2007) 1073-1101.

[57] A. Barth, The infrared absorption of amino acid side chains, Progress in biophysics and molecular biology, 74 (2000) 141-173.

[58] T. Dudler, W.Q. Chen, S. Wang, T. Schneider, R.R. Annand, R.O. Dempcy, R. Crameri, M. Gmachl, M. Suter, M.H. Gelb, High-level expression in Escherichia coli and rapid purification of enzymatically active honey bee venom phospholipase A2, Biochimica et biophysica acta, 1165 (1992) 201-210.

[59] P.J. Yunes Quartino, J.L. Barra, G.D. Fidelio, Cloning and functional expression of secreted phospholipases A(2) from Bothrops diporus (Yarara Chica), Biochemical and biophysical research communications, 427 (2012) 321-325.

[60] W.L. Yang, L.S. Peng, X.F. Zhong, J.W. Wei, X.Y. Jiang, L.T. Ye, L. Zou, H.B. Tu, W.Y. Wu, A.L. Xu, Functional expression and characterization of a recombinant phospholipase A2 from sea snake Lapemis hardwickii as a soluble protein in E. coli, Toxicon : official journal of the International Society on Toxinology, 41 (2003) 713-721.

[61] R. Verger, Pancreatic lipases, in, Elsevier, Amsterdam, 1984, pp. 84-150.

[62] S. Cherif, A. Fendri, N. Miled, H. Trabelsi, H. Mejdoub, Y. Gargouri, Crab digestive lipase acting at high temperature: purification and biochemical characterization, Biochimie, 89 (2007) 1012-1018.

[63] R.A. Demel, W.S. Geurts van Kessel, R.F. Zwaal, B. Roelofsen, L.L. van Deenen, Relation between various phospholipase actions on human red cell membranes and the interfacial phospholipid pressure in monolayers, Biochimica et biophysica acta, 406 (1975) 97-107.

[64] H.M. Verheij, M.C. Boffa, C. Rothen, M.C. Bryckaert, R. Verger, G.H. de Haas, Correlation of enzymatic activity and anticoagulant properties of phospholipase A2, European journal of biochemistry, 112 (1980) 25-32.